Title: Anticancer properties of the fatty acid synthase inhibitor TVB-3166 on oral squamous cell carcinoma cell lines

Running title: Effects of TVB-3166 on OSCC cell lines

Authors: Iara Gonçalves de Aquino[a], Débora Campanella Bastos[a,b], Florence Juana Maria Cuadra-Zelaya[a], Isadora Ferrari Teixeira[a], Tuula Salo[c,d], Ricardo Della Coletta[a], and Edgard Graner[a]

[a] Department of Oral Diagnosis, School of Dentistry of Piracicaba, State University of Campinas (UNICAMP), Piracicaba, Sao Paulo, Brazil

[b] Department of Morphology, School of Dentistry of Piracicaba, State University of Campinas (UNICAMP), Piracicaba, Sao Paulo, Brazil

[c] Cancer and Translational Medicine Research Unit, Faculty of Medicine and Medical Research Center Oulu, Oulu University Hospital, University of Oulu, Oulu, Finland.

[d] Institute of Oral and Maxillofacial Disease, University of Helsinki, and HUSLAB, Department of Pathology, Helsinki University Hospital, Helsinki, Finland.

Corresponding Author: Edgard Graner, Department of Oral Diagnosis, School of Dentistry of Piracicaba, State University of Campinas (UNICAMP), Av. Limeira 901, Areão, Piracicaba 13414-018, São Paulo, Brazil. Phone: 55-19-2106-5318. E-mail: graner@unicamp.br

Abstract

Objective: Fatty acid synthase (FASN) is overexpressed in several human cancers, including oral squamous cell carcinoma (OSCC). TVB-3166 is a recently described FASN inhibitor with antitumor effects and potential clinical relevance. The objective of this study was to evaluate the effects of TVB-3166 on OSCC cell lines.

Materials and methods: The OSCC cell line SCC-9 modified to express ZsGreen (ZsG) (SCC-9 ZsG) and its *in vivo* selected metastatic derivative LN-1A were used to evaluate anticancer properties of TVB-3166. Cell viability was determined using MTT assays and proliferation determined by cell counting in a Neubauer chamber. Cell death and cell cycle progression were analyzed by Annexin V-PE/7-ADD-PerCP labeling and PI staining, respectively. Cell migration was assayed by scratch assays and cell adhesion using myogel. Production of FASN, p-AKT, CPT1-α, and epithelial-mesenchymal transition (EMT) markers were examined by Western blotting.

Results: TVB-3166 significantly reduced cell viability and proliferation, promoted cell cycle arrest and apoptosis, and increased adhesion to myogel in both OSCC cell lines. Finally, the drug reduced SCC-9 ZsG migration.

Conclusion: Our results demonstrated that TVB-3166 has anticancer effects on both SCC-9 ZsG and its metastatic version LN-1A, which are worthy of investigation in preclinical models for OSCC.

Keywords: TVB-3166; fatty acid synthase; oral squamous cell carcinoma; cell lines

1 Introduction

Oral squamous cell carcinoma (OSCC) is the most common type of head and neck malignant tumor and ranked the eighth leading cause of cancer worldwide (Bray et al., 2018). Despite all available therapeutic strategies, including surgery and combination of radio and chemotherapy, the five-year survival rate of OSCC is approximately 50% (Cannon et al., 2017; Warnakulasuriya, 2009). Despite the research efforts worldwide with oral and head and neck squamous cell carcinomas (SCC), there is no effective molecular target for therapy or biomarkers with a predictive value at the moment.

Metabolic reprogramming is the hallmark of tumor progression and metastasis (Hanahan & Weinberg, 2011). In contrast to normal cells, *de novo* lipogenesis is activated in cancer cells, providing selective proliferative and survival advantages (Buckley et al., 2017; Zhan et al., 2008). Fatty acid synthase (FASN), a key enzyme of lipid biosynthesis, is significantly overexpressed in several human malignancies and has been correlated to tumor recurrence, metastasis, chemotherapeutic resistance, and poor prognosis (Röhrig & Schulze, 2016; Witkiewicz et al., 2008; Zeng et al., 2010). In OSCC, FASN expression is essential for cancer cell proliferation and associated with overall survival rates and microscopic characteristics that influence disease progression and prognosis (Agostini et al., 2014; Silva et al., 2008).

Since the ascription of an oncogenic role for FASN, this enzyme has been considered as a potential therapeutic target for cancer treatment (Migita et al., 2009). Experimental studies have shown that FASN pharmacologic inhibition or knockdown reduces cancer cell proliferation, induces apoptosis, and decreases the size of tumor in cancer xenografts (Agostini et al., 2014; Bastos et al., 2017; Chuang, Lee, Lin, Lin, & Hwang, 2019; Javier A. Menendez & Lupu, 2017; Zadra et al., 2019). Moreover, FASN

inhibition with orlistat decreases the number of metastatic cervical lymph nodes in an oral tongue orthotopic model (Agostini et al., 2014). Although currently available FASN inhibitors (e.g. orlistat, cerulenin, and C75) demonstrated clear antitumor activity, their evaluation in clinical trials is hampered by their metabolic and pharmacologic limitations (Flavin, Peluso, Nguyen, & Loda, 2010).

Reversible imidazopyridine-based FASN inhibitors were recently developed by 3-V-Biosciences (TVB-2640, TVB-3166, TVB-3664, TVB-3693, and TVB-3567) and demonstrate antitumor activity *in vitro* and *in vivo* (Benjamin et al., 2015; Heuer et al., 2017; Jafari et al., 2019; Long et al., 2018; Tao et al., 2019; Ventura et al., 2015; Zaytseva et al., 2018). These compounds seem to be better tolerated in mice than the older compounds such as cerulenin, C75, and orlistat, widely used in preclinical studies by several research groups, including ours (Agostini et al., 2014; Bastos et al., 2017; Carvalho et al., 2008; Javier A. Menendez & Lupu, 2017; Seguin et al., 2012). Importantly, TVB-2640 is the first FASN inhibitor to be included in a phase II clinical trial (ClinicalTrials.gov: NCT 03032484, Konkel, Caflisch, Diaz Duque, & Brenner, 2018). Preliminary results demonstrated the tolerability of TVB-2640 with no significant adverse effects in patients with non-small cell lung, ovarian, and breast cancer (Brenner et al., 2015; Dean et al., 2016). On the other hand, TVB-3166 and TVB-3664 has shown antitumor activity in breast, prostate, colorectal, and lung preclinical studies (Heuer et al., 2017; Ventura et al., 2015; Zaytseva et al., 2018). Since TVB-3166 was not tested yet on OSCC, in the present study we evaluate its effects on two OSCC cell lines, the parental SCC-9 ZsG and its *in vivo* selected aggressive and metastatic form LN-1A. Our studies provide the first evidence that TVB-3166 has anticancer properties in OSCC cells by inhibiting viability and proliferation, promoting cell cycle arrest and cell death, and modulating their migration and adhesion.

2 Materials and methods

2.1 Cell culture

SCC-9 cells (American Type Culture Collection – ATCC, Manassas, VA, USA) stably expressing ZsGreen protein (SCC-9 ZsG) were implanted subcutaneously into the footpads of left front limb of BALC/c nude mice and fragments of the metastatic axillary lymph nodes used for explants cultures, from which SCC-9 ZsG LN-1A (LN-1A) cell line was isolated (Agostini et al., 2014). SCC-9 ZsG and LN-1A cells were maintained in DMEM/F-12 (Invitrogen, Carlsbad, CA, USA) supplemented with 2% or 10% of FBS (Cultilab, Campinas, Brazil), 400 ng/mL hydrocortisone and 1% antibiotic/antimycotic solution (Invitrogen) at 37°C in a humidified atmosphere with 5% CO_2. TVB-3166 (**Fig. 1**A, Sigma, St Louis, MO, USA) and dimethylsulfoxide - DMSO (Sigma) as control were added to the culture medium at the concentrations described in the figure legends.

2.2 Cell viability and proliferation assays

Cell viability was measured using (4,5-dimethylthiazol-2-yl) -2,5 diphenyltetrazolium bromide - MTT (Sigma) after incubation of SCC-9 ZsG and LN-1A cells with DMEM/F-12 supplemented with 2% FBS containing increasing doses of TVB-3166 for 48 h. The IC_{50} values were determined through the dose-effect curve with the aid of CompuSyn software (Cambridge, MA, USA). In order to evaluate proliferation, 8 x 10^3 cells were seeded in each well of 24-well plates with DMEM/F-12 containing 10% FBS. Following incubation for more 24 h in serum-free medium, cells were cultured for 24, 48, and 72 h in medium containing 2% FBS plus TVB-3166, trypsinized, and counted in a Neubauer chamber from triplicate wells. The experiments were performed three times independently.

2.3 Flow cytometry

Samples were analyzed in FACSCalibur flow cytometer (BD Biosciences, San Jose, CA, USA) equipped with an argon laser. Ten thousand events were collected for each sample. Previously, cells were seeded in T-25 culture flasks, serum starved for 24 h, and treated with TVB-3166 in DMEM/F12 containing 2% FBS for 48 h. For the analysis of cell death, cells were washed with PBS and resuspended in a binding buffer containing Annexin V-PE and 7-AAD-PerCP (1:100, BD Biosciences Pharmingen). Apoptosis was quantified by the number of Annexin V-PE positive cells while necrosis by positivity for 7-AAD-PerCP using the CellQuest software (Becton Dickinson and Company, San Jose, CA, USA). For the cell cycle analysis, after fixation in cold 70% ethanol, cells were treated with RNAse (10 µg/mL) during 1 h at 37 °C and stained with 50 µg/mL of propidium iodide for 2 h at 4 °C. The distribution of cells in the cell cycle was analyzed with the software ModFit (Verity Software House).

2.4 Scratch assays

Cell migration was assayed by measuring the time required by cells to migrate into a wound produced on the surface of a confluent layer of cells (Liang, Park, & Guan, 2007; Mendonça et al., 2017). A total of 2 x 10^5 cells grown in DMEM/F-12 with 10% FBS were plated in each well of 24-well plates. After 24 h, the confluent monolayer was scraped with a sterile 200 µL pipette tip to create cell-free areas. After three washes with PBS, medium supplemented with 2% FBS containing TVB-3166 was added and cells incubated for additional 24 h. Images were obtained using a Nikon Eclipse Ti-S microscope. Cell migration was calculated with Image J software (National Institute of Health, Bethesda, Maryland, USA) and expressed as the percentage of wound closure.

2.5 Adhesion assay

Cell adhesion assay was performed using myogel, a human uterine leiomyoma-derived matrix (Salo et al., 2015). Wells from 48-well culture plates were coated with 10 μg/μL of myogel in PBS at 4 °C for 24 h. Control wells were coated with PBS only. Next, the same wells were washed three times with PBS and incubated with 3% bovine serum albumin (BSA, Sigma) for 2 h at 37 °C. Subconfluent SCC-9 ZsG or LN-1A cells were incubated in DMEM/F-12 supplemented with 2% FBS plus TVB-3166 for 48 h, harvested, plated (8×10^4 cells per well) in the pre-coated wells, and incubated at 37 °C in a humidified atmosphere with 5% CO_2 for 1 hour. Non-adherent cells were washed away and the remaining adherent cells fixed in 10% trichloroacetic acid (TCA, Sigma), stained with 0,1% crystal violet, and quantified using an ELISA reader at 595 nm (Bio-Rad, Hercules, CA, USA). Cell adhesion to BSA-coated wells served as negative controls.

2.6 Protein extraction and Western blotting

Protein lysates from cells for Western blotting reactions were performed as previously described (Carvalho et al., 2008). Fifty micrograms of each protein lysate were probed with primary antibodies against FASN (1:3000, BD Biosciences), p-Akt S473 (1:1000), CPT1-α (1:1000), E-cadherin (1:1000), N-cadherin (1:1000), vimentin (1:1000), and Snail (1:500), all purchased from Cell Signaling Technology (Danvers, MA, USA). Primary antibody against β-actin (1:30,000, Sigma) was used as the loading controls. Densitometry was performed with the aid of the Image J software and the values normalized by β-actin.

3 Results

3.1 TVB-3166 inhibits viability and growth of OSCC cells

In order to evaluate the effect of TVB-3166 on the viability of the studied OSCC cell lines, we treated both SCC-9 ZsG and LN-1A cells with the concentrations of 10, 25, 50, 75, and 100 μM in the culture medium supplemented with 2% FBS for 48 h. As expected, the drug significantly reduced the viability of both cell lines in a dose-dependent manner (**Fig. 1**B–C). Next, after the calculation of IC_{50} values for each cell line (30 and 37 μM for SCC-9 ZsG and LN-1A, respectively), we checked whether TVB-3166 inhibits their proliferation. In fact, TVB-3166 significantly inhibited the growth of SCC-9 ZsG cells after 48 and 72 h at 30 (IC_{50}) and 15 μM, whereas metastatic LN-1A cells had their proliferation inhibited after 72 h at 37 μM (IC_{50}) only (**Fig. 1**E–F). Cell morphology was also changed by the treatment with TVB-3166. As shown in **Fig. 1**D, the drug altered the typical polygonal morphology of control SCC-9 ZsG and LN-1A cells to a predominantly fusiform phenotype with numerous cytoplasmic extensions. Next, to assess the effects of TVB-3166 on the amount of FASN and carnitine palmitoyltransferase 1 alpha (CPT1-α), enzyme that catalyzes the translocation of long-chain fatty acids across the mitochondrial membrane and favors their oxidation, as well as on the activation of the AKT oncogenic pathway, we performed Western blotting reactions with protein lysates prepared from the studied cell lines treated with the drug or its vehicle. As depicted in **Fig. 1**G, the incubation with TVB-3166 did not modify the amount of FASN and CPT1-α, however, the latter was more abundant in SCC-9 ZsG than in metastatic LN-1A cells. Importantly, TVB-3166 considerably decreased the amount of phosphorylated AKT in both cell lines, which was more drastic in LN-1A cells (**Fig. 1**G–I).

3.2 TVB-3166 promotes G0/G1 cell cycle arrest and death of OSCC cells

To better characterize the antiproliferative properties of TVB-3166 on OSCC cells, we next performed flow cytometry experiments, which showed an increase in the number of cells in G0-G1 and, concomitantly, a clear reduction of the S phase in both SCC-9 ZsG and LN-1A cells (**Fig. 2**A–B). To verify whether TVB-3166 induce cell death, we performed Annexin-V-PE and 7-ADD-PerCP labeling. As shown in **Fig. 2**C–D, Annexin V-PE positive SCC-9 ZsG and LN-1A cells were significantly increased after the treatments in comparison with control cells. Despite the fact that positivity of both cell lines was lower for 7-AAD-PerCP than for Annexin-V-PE, a significant increase of necrotic SCC-9 ZsG cells was observed after exposure to TVB-3166, which was not observed in metastatic LN-1A cells **(Fig. 2**E–F).

3.3 TVB-3166 changes migration and adhesion of OSCC cells

Since EMT has been described in OSCC cells and promotes a migratory and invasive phenotype (Thierauf, Veit, & Hess, 2017), we next searched whether TVB-3166 modifies the migration and adhesion of the studied cell lines. As shown in **Fig. 3**A, TVB-3166 significantly decreased SCC-9 ZsG cell migration in comparison with control cells. In contrast, the drug did not change the migratory capacity of the metastatic LN-1A cells (**Fig. 3**B). In order to evaluate the effect of this drug on cell adhesion, we utilized myogel, a tumor-derived extracellular matrix which mimics, at least in part, the microenvironment of human solid cancers (Salo et al., 2015). Interestingly, our results demonstrated that TVB-3166 strongly increases the adhesion of both SCC-9 ZsG and LN-1A cells to myogel in comparison with the control cells (**Fig. 3**C–D). Finally, we searched for EMT markers in protein lysates obtained from SCC-9 ZsG and LN-1A cells treated or not with TVB-3166. As depicted in **Fig. 3**E, no drastic alterations were observed except from an

increase of E-cadherin levels in both cell lines and increased N-cadherin and vimentin amount in SCC-9 ZsG cell lysates.

4 Discussion

Our group has previously shown the antitumor properties of the FASN inhibitor orlistat in both OSCC and melanoma models (Agostini et al., 2014; Bastos et al., 2017; Carvalho et al., 2008; Seguin et al., 2012). This drug was originally described as an inhibitor of pancreatic and gastric lipases and clinically applied for the treatment of obesity (Heck, Yanovski, & Calis, 2000). When employed in an orthotopic oral tongue SCC, orlistat strongly inhibited both primary tumor growth and regional lymph node colonization (43%) due to, at least in part, cell cycle arrest and induction of apoptosis (Agostini et al., 2014). Orlistat has been used as a tool for FASN inhibition in several laboratories and shown significant *in vitro* and *in vivo* antitumor effects (Chuang et al., 2019; Kridel, Axelrod, Rozenkrantz, & Smith, 2004; J. A. Menendez, Vellon, & Lupu, 2005), however, it has low chances to be clinically tested due to its pharmacological characteristics, such as low cell permeability, lack of selectivity, poor oral bioavailability and metabolic stability (Flavin et al., 2010). On the other hand, when conjugated with nanoparticles, orlistat showed improved solubility and cytotoxicity as well as synergistic effects with taxanes in prostate cancer cells (Souchek et al., 2017).

New perspectives to make FASN inhibition an option to be tested in humans arose from the development of new compounds such as the TVB family, from which TVB-2640 is already included in a clinical trial with non-small cell lung, ovarian, and breast cancer patients (ClinicalTrials.gov: NCT 02223247), and IPI-9119, that was shown to reduce growth of castration-resistant prostate cancer (CRPC) xenografts and human metastatic CRPC-derived organoids (Zadra et al., 2019). In the search for a FASN inhibitor with potential to be included in future human OSCC chemotherapy protocols,

herein we assessed the effects of the recently developed FASN inhibitor TVB-3166 on cell lines obtained from primary (SCC-9 ZsG) oral tongue SCC or *in vivo* selected (LN-1A) from metastatic lymph nodes colonized by SCC-9 ZsG cells. This drug was the only commercially available inhibitor from the TVB family in the beginning of the present study.

We demonstrated that TVB-3166 significantly reduces the viability and proliferation of both SCC-9 ZsG and LN-1A cells, which showed IC_{50} values slightly higher for the latter. TVB-3166 has shown consistent antiproliferative and proapoptotic effects in cells derived from prostate, breast, colon, lung, ovarian and bladder cancers (Tao et al., 2019; Ventura et al., 2015). Concurrently, inhibition of metabolic and signal transduction pathways critical for cell growth, proliferation, and survival, including PI3K-AKT-mTOR and β-catenin was also evident in lung, colon, ovary, and breast cancer cells (Ventura et al., 2015). Indeed, in the present report, TVB-3166 decreased the activation of AKT in both studied OSCC cell lines, suggesting a similar mechanism of action. AKT activation is associated with enhanced invasiveness and EMT induction by down regulating the expression of E-cadherin in OSCC cell lines (Grille et al., 2003). The AKT pharmacological inhibitor MK-2209 reduces migration *in vitro*, the size of primary tumors, and cervical metastasis in orthotopic tongue model of OSCC (Knowles et al., 2011). Previous work showing that FASN inhibition with cerulenin and its synthetic derivative C75 stimulates fatty acid oxidation by activating CPT1-α and promoting weight loss in mice raised concerns about their translational relevance (Loftus, 2000). In addition, fatty acid oxidation mediated by CPT1-α seem to contribute to cell survival and its inhibition suppresses of cancer cell proliferation (Melone et al., 2018). In our hands TVB-3166 did not change the amount of CPT1-α in SCC-9ZsG and LN-1A cell lysates.

Uncontrolled cell proliferation and escape from cell death are hallmarks of cancer (Hanahan & Weinberg, 2011). Here, we show that TVB-3166 efficiently promotes G0/G1 cell cycle arrest in both studied OSCC cell lines, which was slightly more efficient in the metastatic LN-1A (46.1%) than in SCC-9 ZsG (40.09%). The effects of TVB-3166 on cell cycle progression of cancer cells were not yet described, however, previous studies reported that the drug modulates the expression of genes that control cell cycle, such as *CCNA1*, *CCNB2*, *CDK1*, and *CDK2* (Ventura et al., 2015). We also found that TVB-3166 promotes apoptosis in both studied cell lines and necrosis in SCC-9 ZsG cells. TVB-3166-induced apoptotic cell death was already described in lung, prostate, and bladder cancer cells (Tao et al., 2019; Ventura et al., 2015).

In our studies, we demonstrated that TVB-3166 significantly reduces SCC-9 ZsG cell migration, however, does not change the migratory ability of the metastatic LN-1A cells. In fact, the latter produces significantly more vimentin than the former, in agreement with its highly metastatic capability in orthotopic mouse model (unpublished data). Vimentin was found as the most upregulated gene in metastatic OSCC cells in comparison with non-metastatic cells and its expression essential for the increased migration activity of tumor cells (Liu et al., 2016). Despite the slightly increased e-cadherin production by both SCC-9 ZsG and LN-1A cells as well as vimentin amount in SCC-9 ZsG cells, TVB-3166 did not significantly modulate EMT markers. It is possible that the inhibition of SCC-9 ZsG migration occurs through a vimentin independent pathway. Moreover, the stable FASN knockdown reduces metastasis by inhibiting cell migration and TVB-3664, an analog of TVB-3166, leads to suppression of colorectal cancer cell growth, migration, and invadopodia formation by decreasing activation of p-MET, p-FAK, and p-PAX (Jafari et al., 2019; Zaytseva et al., 2012). Herein, TVB-3166 increased the adhesion of both SCC-9 ZsG and LN-1A cells to myogel, a matrix prepared

from human uterine leiomyoma tissue (Salo et al., 2015). Likewise, we have previously observed that the adhesion of mouse metastatic melanoma cells (B16-F10) to laminin is increased by the treatment with both orlistat and cerulenin (unpublished data). The implications of these findings for OSCC growth and metastasis require additional investigation. Yet, in concert with the increased e-cadherin production by SCC-9 ZsG and LN-1A cells following the treatment with TVB-3166, it is possible to hypothesize that enhanced cell-to-cell and cell-matrix adhesion play a role in the anticancer properties of FASN inhibitors. In fact, clay nanoparticles were shown to enhance adhesion to fibronectin and delay breast cancer cell migration (Abduljauwad & Ahmed, 2019). Additionally, the β-adrenergic agonist salbutamol enhances adhesion to matrigel, diminishes breast cancer cell migration, and reduces experimental lung metastases in a xenograft model (Rivero et al., 2017).

Taken together, the results here presented show that TVB-3166 has anticancer effects on OSCC cell lines which, if confirmed by future preclinical studies, may provide the basis for its inclusion (or inclusion of TVB-2640) in clinical trials in association with classical chemotherapy indicated for OSCC.

Acknowledgements

This work was supported by the Fundação de Amparo à Pesquisa do Estado de São Paulo (FAPESP, 2014/20832-3), Coordenação de Aperfeiçoamento de Pessoal de Nível Superior – Brasil (CAPES) – Finance Code 001, and Conselho Nacional Nacional de Desenvolvimento Científico e Tecnológico (CNPq, 303064/2018-8). The authors thank Marco A. Cavallari Jr for the drawing of Fig. 1A.

Conflict of interest

The authors declare no conflicts of interest.

References

Abduljauwad, S. N., & Ahmed, H. ur R. (2019). Enhancing cancer cell adhesion with clay nanoparticles for countering metastasis. *Scientific Reports*. https://doi.org/10.1038/s41598-019-42498-y

Agostini, M., Almeida, L. Y., Bastos, D. C., Ortega, R. M., Moreira, F. S., Seguin, F., … Graner, E. (2014). The fatty acid synthase inhibitor orlistat reduces the growth and metastasis of orthotopic tongue oral squamous cell carcinomas. *Molecular Cancer Therapeutics*. https://doi.org/10.1158/1535-7163.MCT-12-1136

Bastos, D. C., Paupert, J., Maillard, C., Seguin, F., Carvalho, M. A., Agostini, M., … Graner, E. (2017). Effects of fatty acid synthase inhibitors on lymphatic vessels: an in vitro and in vivo study in a melanoma model. *Laboratory Investigation*. https://doi.org/10.1038/labinvest.2016.125

Benjamin, D. I., Li, D. S., Lowe, W., Heuer, T., Kemble, G., & Nomura, D. K. (2015). Diacylglycerol metabolism and signaling is a driving force underlying FASN inhibitor sensitivity in cancer cells. *ACS Chemical Biology*, *10*(7), 1616–1623. https://doi.org/10.1021/acschembio.5b00240

Bray, F., Ferlay, J., Soerjomataram, I., Siegel, R. L., Torre, L. A., & Jemal, A. (2018). Global cancer statistics 2018: GLOBOCAN estimates of incidence and mortality worldwide for 36 cancers in 185 countries. *CA: A Cancer Journal for Clinicians*, *68*(6), 394–424. https://doi.org/10.3322/caac.21492

Brenner, A., Infante, J., Patel, M., Arkenau, H.-T., Voskoboynik, M., Borazanci, E., … Burris, H. A. (2015). Abstract A54: first-in-human study of the first-in-class fatty acid synthase (FASN) inhibitor, TVB-2640 as monotherapy or in combination - final results of dose escalation. In *Clinical Trials* (pp. A54–A54). American Association for Cancer Research. https://doi.org/10.1158/1535-7163.TARG-15-A54

Buckley, D., Duke, G., Heuer, T. S., O'Farrell, M., Wagman, A. S., McCulloch, W., & Kemble, G. (2017). Fatty acid synthase – modern tumor cell biology insights into a classical oncology target. *Pharmacology & Therapeutics*, *177*, 23–31. https://doi.org/10.1016/j.pharmthera.2017.02.021

Cannon, R. B., Sowder, J. C., Buchmann, L. O., Hunt, J. P., Hitchcock, Y. J., Lloyd, S., … Monroe, M. M. (2017). Increasing use of nonsurgical therapy in advanced-stage oral cavity cancer: a population-based study. *Head & Neck*, *39*(1), 82–91. https://doi.org/10.1002/hed.24542

Carvalho, M. A., Zecchin, K. G., Seguin, F., Bastos, D. C., Agostini, M., Rangel, A. L. C. A., … Graner, E. (2008). Fatty acid synthase inhibition with orlistat promotes apoptosis and reduces cell growth and lymph node metastasis in a mouse melanoma model. *International Journal of Cancer*. https://doi.org/10.1002/ijc.23835

Chuang, H.-Y., Lee, Y.-P., Lin, W.-C., Lin, Y.-H., & Hwang, J.-J. (2019). Fatty acid inhibition sensitizes androgen-dependent and -independent prostate cancer to radiotherapy via FASN/NF-κB Pathway. *Scientific Reports*, *9*(1), 13284. https://doi.org/10.1038/s41598-019-49486-2

Dean, E. J., Falchook, G. S., Patel, M. R., Brenner, A. J., Infante, J. R., Arkenau, H.-T., … Burris, H. (2016). Preliminary activity in the first in human study of the first-in-class fatty acid synthase (FASN) inhibitor, TVB-2640. *Journal of Clinical Oncology*, *34*(15_suppl), 2512–2512. https://doi.org/10.1200/JCO.2016.34.15_suppl.2512

Flavin, R., Peluso, S., Nguyen, P. L., & Loda, M. (2010). Fatty acid synthase as a potential therapeutic target in cancer. *Future Oncology*, *6*(4), 551–562. https://doi.org/10.2217/fon.10.11

Grille, S. J., Bellacosa, A., Upson, J., Klein-Szanto, A. J., Van Roy, F., Lee-Kwon, W., … Larue, L. (2003). The protein kinase Akt induces epithelial mesenchymal transition and promotes enhanced motility and invasiveness of squamous cell carcinoma lines. *Cancer Research*.

Hanahan, D., & Weinberg, R. A. (2011). Hallmarks of cancer: the next generation. *Cell*, *144*(5), 646–674. https://doi.org/10.1016/j.cell.2011.02.013

Heck, A. M., Yanovski, J. A., & Calis, K. A. (2000). Orlistat, a new lipase inhibitor for the management of obesity. *Pharmacotherapy*. https://doi.org/10.1592/phco.20.4.270.34882

Heuer, T. S., Ventura, R., Mordec, K., Lai, J., Fridlib, M., Buckley, D., & Kemble, G. (2017). FASN inhibition and taxane treatment combine to enhance anti-tumor efficacy in diverse xenograft tumor models through disruption of tubulin palmitoylation and microtubule organization and FASN inhibition-mediated effects on oncogenic signaling and gene expression. *EBioMedicine*, *16*, 51–62. https://doi.org/10.1016/j.ebiom.2016.12.012

Jafari, N., Drury, J., Morris, A. J., Onono, F. O., Stevens, P. D., Gao, T., … Zaytseva, Y. Y. (2019). De novo fatty acid synthesis-driven sphingolipid metabolism promotes metastatic potential of colorectal cancer. *Molecular Cancer Research*, *17*(1), 140–152. https://doi.org/10.1158/1541-7786.MCR-18-0199

Knowles, J. A., Golden, B., Yan, L., Carroll, W. R., Helman, E. E., & Rosenthal, E. L. (2011). Disruption of the AKT pathway inhibits metastasis in an orthotopic model of head and neck squamous cell carcinoma. *Laryngoscope*. https://doi.org/10.1002/lary.22180

Konkel, B., Caflisch, L., Diaz Duque, A. E., & Brenner, A. J. (2018). Actr-25: updated results from a prospective, randomized phase 2 study in patients with first relapse of high-grade astrocytoma using TVB-2640 in combination with avastin versus avastin alone. *Neuro-Oncology*, *20*(suppl_6), vi16–vi16. https://doi.org/10.1093/neuonc/noy148.058

Kridel, S. J., Axelrod, F., Rozenkrantz, N., & Smith, J. W. (2004). Orlistat is a novel inhibitor of fatty acid synthase with antitumor activity. *Cancer Research*.

Liang, C.-C., Park, A. Y., & Guan, J.-L. (2007). In vitro scratch assay: a convenient and inexpensive method for analysis of cell migration in vitro. *Nature Protocols*, *2*(2), 329–333. https://doi.org/10.1038/nprot.2007.30

Liu, S., Liu, L., Ye, W., Ye, D., Wang, T., Guo, W., … Zhang, Z. (2016). High vimentin expression associated with lymph node metastasis and predicated a poor prognosis in oral squamous cell carcinoma. *Scientific Reports*, *6*(1), 38834. https://doi.org/10.1038/srep38834

Loftus, T. M. (2000). Reduced food intake and body weight in mice treated with fatty acid synthase inhibitors. *Science*, *288*(5475), 2379–2381. https://doi.org/10.1126/science.288.5475.2379

Long, R., Zhang, L., Shi, L., Shen, Y., Hu, F., Zeng, C., & Min, W. (2018). Two-color vibrational imaging of glucose metabolism using stimulated Raman scattering. *Chemical Communications*, *54*(2), 152–155. https://doi.org/10.1039/C7CC08217G

Melone, M. A. B., Valentino, A., Margarucci, S., Galderisi, U., Giordano, A., & Peluso, G. (2018). The carnitine system and cancer metabolic plasticity. *Cell Death & Disease*, *9*(2), 228. https://doi.org/10.1038/s41419-018-0313-7

Mendonça, B. dos S., Agostini, M., Aquino, I. G., Dias, W. B., Bastos, D. C., & Rumjanek, F. D. (2017). Suppression of MAGE-A10 alters the metastatic phenotype of tongue squamous cell carcinoma cells. *Biochemistry and Biophysics Reports*. https://doi.org/10.1016/j.bbrep.2017.04.009

Menendez, J. A., Vellon, L., & Lupu, R. (2005). Antitumoral actions of the anti-obesity drug orlistat (Xenical^{TM}) in breast cancer cells: blockade of cell cycle progression, promotion of apoptotic cell death and PEA3-mediated transcriptional repression of Her2/neu (ERBB-2) oncogene. *Annals of Oncology*, *16*(8), 1253–1267. https://doi.org/10.1093/annonc/mdi239

Menendez, Javier A., & Lupu, R. (2017). Fatty acid synthase (FASN) as a therapeutic target in breast cancer. *Expert Opinion on Therapeutic Targets*, *21*(11), 1001–1016. https://doi.org/10.1080/14728222.2017.1381087

Migita, T., Ruiz, S., Fornari, A., Fiorentino, M., Priolo, C., Zadra, G., … Loda, M. (2009). Fatty acid synthase: a metabolic enzyme and candidate oncogene in prostate cancer. *JNCI: Journal of the National Cancer Institute*, *101*(7), 519–532. https://doi.org/10.1093/jnci/djp030

Rivero, E. M., Piñero, C. P., Gargiulo, L., Entschladen, F., Zänker, K., Bruzzone, A., & Lüthy, I. A. (2017). The β2-adrenergic agonist salbutamol inhibits migration, invasion and metastasis of the human breast cancer MDA-MB-231 cell line. *Current Cancer Drug Targets*, *17*(8). https://doi.org/10.2174/1568009617666170330151415

Röhrig, F., & Schulze, A. (2016). The multifaceted roles of fatty acid synthesis in cancer. *Nature Reviews Cancer*, *16*(11), 732–749. https://doi.org/10.1038/nrc.2016.89

Salo, T., Sutinen, M., Hoque Apu, E., Sundquist, E., Cervigne, N. K., de Oliveira, C. E., … Coletta, R. D. (2015). A novel human leiomyoma tissue derived matrix for cell culture studies. *BMC Cancer*, *15*(1), 981. https://doi.org/10.1186/s12885-015-1944-z

Seguin, F., Carvalho, M. A., Bastos, D. C., Agostini, M., Zecchin, K. G., Alvarez-Flores, M. P., … Graner, E. (2012). The fatty acid synthase inhibitor orlistat reduces experimental metastases and angiogenesis in B16-F10 melanomas. *British Journal of Cancer*, *107*(6), 977–987. https://doi.org/10.1038/bjc.2012.355

Silva, S., Perez, D., Nishimoto, I., Alves, F., Pinto, C., Kowalski, L., & Graner, E. (2008). Fatty acid synthase expression in squamous cell carcinoma of the tongue: clinicopathological findings. *Oral Diseases*, *14*(4), 376–382. https://doi.org/10.1111/j.1601-0825.2007.01395.x

Tao, T., Su, Q., Xu, S., Deng, J., Zhou, S., Zhuang, Y., … Yang, X. (2019). Down□regulation of PKM2 decreases FASN expression in bladder cancer cells through AKT/mTOR/SREBP□1c axis. *Journal of Cellular Physiology*, *234*(3), 3088–3104. https://doi.org/10.1002/jcp.27129

Thierauf, J., Veit, J., & Hess, J. (2017). Epithelial-to-mesenchymal transition in the pathogenesis and therapy of head and neck cancer. *Cancers*, *9*(12), 76. https://doi.org/10.3390/cancers9070076

Ventura, R., Mordec, K., Waszczuk, J., Wang, Z., Lai, J., Fridlib, M., … Heuer, T. S. (2015). Inhibition of de novo palmitate synthesis by fatty acid synthase induces apoptosis in tumor cells by remodeling cell membranes, inhibiting signaling pathways, and reprogramming gene expression. *EBioMedicine*, *2*(8), 808–824. https://doi.org/10.1016/j.ebiom.2015.06.020

Warnakulasuriya, S. (2009). Global epidemiology of oral and oropharyngeal cancer. *Oral Oncology*, *45*(4–5), 309–316. https://doi.org/10.1016/j.oraloncology.2008.06.002

Witkiewicz, A. K., Nguyen, K. H., Dasgupta, A., Kennedy, E. P., Yeo, C. J., Lisanti, M. P., & Brody, J. R. (2008). Co-expression of fatty acid synthase and caveolin-1 in pancreatic ductal adenocarcinoma: Implications for tumor progression and clinical outcome. *Cell Cycle*. https://doi.org/10.4161/cc.7.19.6719

Zadra, G., Ribeiro, C. F., Chetta, P., Ho, Y., Cacciatore, S., Gao, X., … Loda, M. (2019). Inhibition of de novo lipogenesis targets androgen receptor signaling in castration-resistant prostate cancer. *Proceedings of the National Academy of Sciences of the United States of America*. https://doi.org/10.1073/pnas.1808834116

Zaytseva, Y. Y., Rychahou, P. G., Gulhati, P., Elliott, V. A., Mustain, W. C., O'Connor, K., … Evers, B. M. (2012). Inhibition of fatty acid synthase attenuates CD44-associated signaling and reduces metastasis in colorectal cancer. *Cancer Research*, *72*(6), 1504–1517. https://doi.org/10.1158/0008-5472.CAN-11-4057

Zaytseva, Y. Y., Rychahou, P. G., Le, A.-T., Scott, T. L., Flight, R. M., Kim, J. T., … Evers, M. (2018). Preclinical evaluation of novel fatty acid synthase inhibitors in primary colorectal cancer cells and a patient-derived xenograft model of colorectal cancer. *Oncotarget*, *9*(37). https://doi.org/10.18632/oncotarget.25361

Zeng, L., Biernacka, K. M., Holly, J. M. P., Jarrett, C., Morrison, A. A., Morgan, A., … Perks, C. M. (2010). Hyperglycaemia confers resistance to chemotherapy on breast cancer cells: the role of fatty acid synthase. *Endocrine-Related Cancer*, *17*(2), 539–551. https://doi.org/10.1677/ERC-09-0221

Zhan, Y., Ginanni, N., Tota, M. R., Wu, M., Bays, N. W., Richon, V. M., … Krauss, S. (2008). Control of cell growth and survival by enzymes of the fatty acid synthesis pathway in HCT-116 colon cancer cells. *Clinical Cancer Research*. https://doi.org/10.1158/1078-0432.CCR-07-5074

Figure legends

Figure 1 - TVB-3166 inhibits viability and growth of OSCC cells. (A) TVB-3166 chemical structure. MTT experiments showing that the treatment with increasing concentrations of TVB-3166 reduces the viability of both SCC-9 ZsG (B) and LN-1A (C) cells in a dose-dependent manner. TVB-3166 changes the phenotype of both SCC-9 ZsG and LN-1A cells in subconfluent monolayers from a predominantly polygonal to a more fusiform appearance, with evident cytoplasmic extensions (D). The treatment with this drug for 48 and 72 h inhibits SCC-9 ZsG (E) and LN-1A (F) cell proliferation, effect that was stronger in the latter after 72 h. (G) The production of FASN, p-AKT, and CPT1-α was analyzed by Western blotting in protein lysates prepared from SCC-9 ZsG and LN-1A cells treated or not with TVB-3166. The drug did not modify the amount of FASN and CPT1-α in both cell lines while p-AKT levels were clearly reduced by TVB-3166, mainly in LN-1A cells (H-I). C: control, (B-C) *p<0.05, **p<0.01, ***p<0.001, Anova and Dunnett test, (D) Phase contrast microscopy, original magnification: 100X, (E-F) *p<0.05, ##p<0.01 for 30 μM, ***p<0.001 Anova and Bonferroni test, (H–I) * p<0.05, *** p<0.001, Anova and Tukey's test.

Figure 2 – TVB-3166 promotes cell cycle arrest and death of OSCC cells. (A–B) Cell cycle analysis by flow cytometry shows that TVB-3166 significantly reduced the percentage of SCC-9 ZsG and LN-1A cells in the S phase and promoted their accumulation in G0/G1. The staining with Annexin V-PE and 7-AAD-PerCP shows that the drug induces apoptotic cell death in both studied cell lines and necrosis in SCC-9 ZsG (C–F). C: control, (A) ***p<0.001 for S and ###p<0.001 for G0/G1, Anova and Tukey's test, (C–F) *p<0.05, Anova and Tukey's test.

Figure 3 – TVB-3166 inhibits migration of SCC-9 ZsG cells and increases adhesion of both SCC-9 ZsG and LN-1A cells. The treatment for 24 h with TVB-3166 significantly reduced SCC-9 ZsG cell migration in comparison with control cells (A) and has no influence on metastatic LN-1A cells (B). TVB-3166 significantly enhanced the adhesion of both SCC-9 ZsG and LN-1A cells to myogel in comparison with the control cells (C–D). (E) Western blotting analysis with protein lysates from SCC-9 ZsG and LN-1A cells treated or not with TVB-3166 shows that e-cadherin levels were increased in both cell lines whereas n -cadherin and vimentin bands enhanced by the treatments in SCC-9 ZsG cells only. C: control, (A–D) Original magnificantion 40X, *$p<0.05$, **$p<0.01$, Anova and Tukey's test.

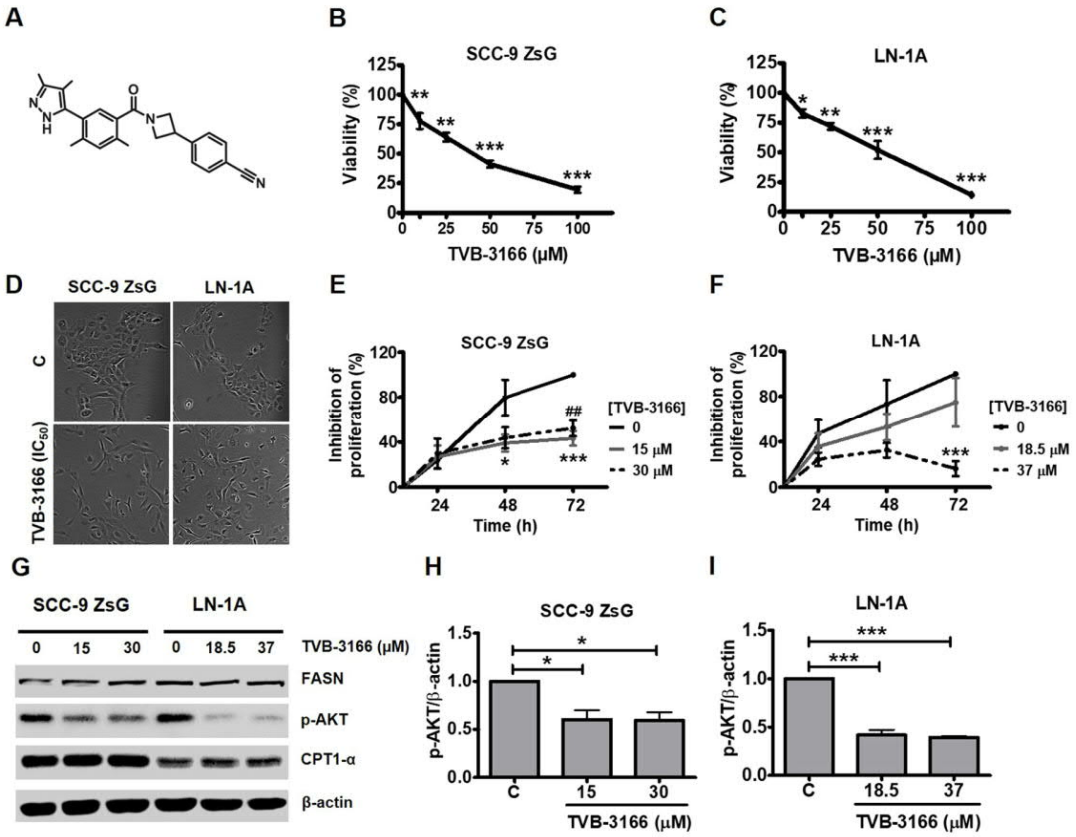
A
B
SCC-9 ZsG
Viability (%)
TVB-3166 (μM)
C
LN-1A
Viability (%)
TVB-3166 (μM)
D
SCC-9 ZsG
LN-1A
C
TVB-3166 (IC50)
E
SCC-9 ZsG
Inhibition of proliferation (%)
Time (h)
[TVB-3166]
0
15 μM
30 μM
F
LN-1A
Inhibition of proliferation (%)
Time (h)
[TVB-3166]
0
18.5 μM
37 μM
G
SCC-9 ZsG
LN-1A
0 15 30 0 18.5 37
TVB-3166 (μM)
FASN
p-AKT
CPT1-α
β-actin
H
SCC-9 ZsG
p-AKT/β-actin
C 15 30
TVB-3166 (μM)
I
LN-1A
p-AKT/β-actin
C 18.5 37
TVB-3166 (μM)

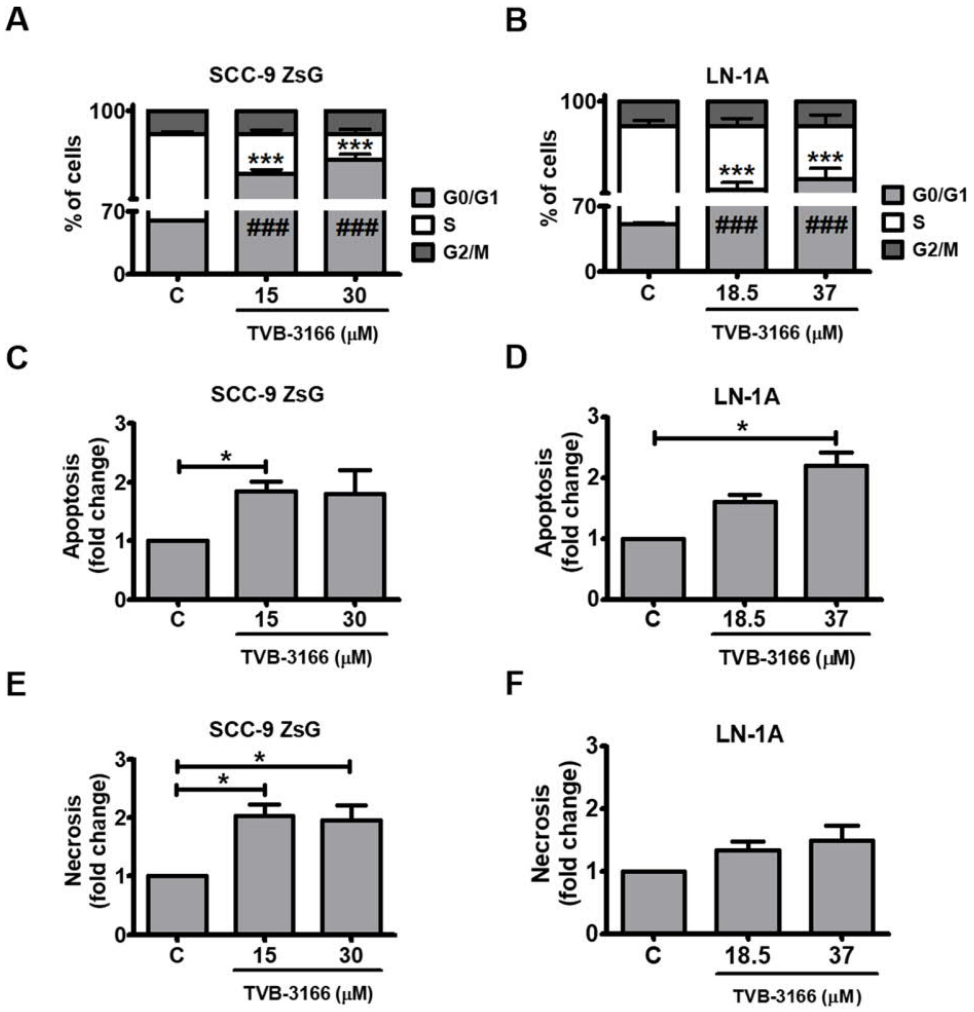
A
SCC-9 ZsG
% of cells
100
70
0
***
***
###
###
G0/G1
S
G2/M
C
15
30
TVB-3166 (μM)
B
LN-1A
% of cells
100
70
0
***
***
###
###
G0/G1
S
G2/M
C
18.5
37
TVB-3166 (μM)
C
SCC-9 ZsG
Apoptosis (fold change)
*
C
15
30
TVB-3166 (μM)
D
LN-1A
Apoptosis (fold change)
*
C
18.5
37
TVB-3166 (μM)
E
SCC-9 ZsG
Necrosis (fold change)
*
*
C
15
30
TVB-3166 (μM)
F
LN-1A
Necrosis (fold change)
C
18.5
37
TVB-3166 (μM)

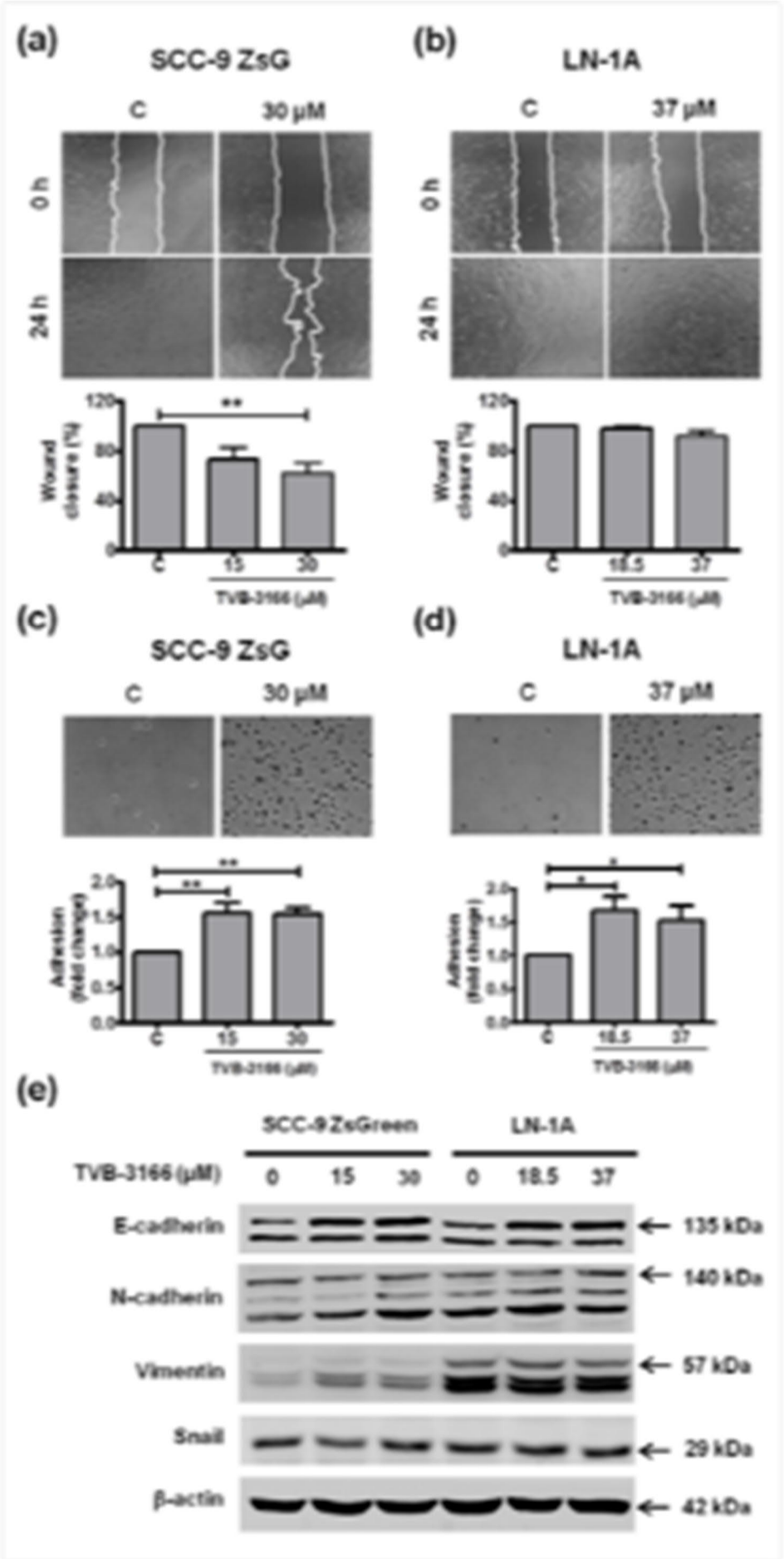
(a)
SCC-9 ZsG
C
30 μM
0 h
24 h
Wound closure (%)
120
80
40
0
**
C
15
30
TVB-3166 (μM)
(b)
LN-1A
C
37 μM
0 h
24 h
Wound closure (%)
120
80
40
0
C
18.5
37
TVB-3166 (μM)
(c)
SCC-9 ZsG
C
30 μM
Adhesion (fold change)
2.0
1.5
1.0
0.5
0.0
**
**
C
15
30
TVB-3166 (μM)
(d)
LN-1A
C
37 μM
Adhesion (fold change)
2.0
1.5
1.0
0.5
0.0
*
*
C
18.5
37
TVB-3166 (μM)
(e)
SCC-9 ZsGreen
LN-1A
TVB-3166 (μM)
0
15
30
0
18.5
37
E-cadherin
135 kDa
N-cadherin
140 kDa
Vimentin
57 kDa
Snail
29 kDa
β-actin
42 kDa